

Quantum Phase Transitions in Odd-Mass Nuclei

A. Leviatan

*Racah Institute of Physics, The Hebrew University,
Jerusalem 91904, Israel
E-mail: ami@phys.huji.ac.il*

D. Petrellis

*Institute of Nuclear Physics, N.C.S.R. "Demokritos",
GR-15310 Aghia Paraskevi, Attiki, Greece
E-mail: petrellis@inp.demokritos.gr*

F. Iachello

*Center for Theoretical Physics, Sloane Physics Laboratory, Yale University,
New Haven, Connecticut 06520-8120, USA
E-mail: francesco.iachello@yale.edu*

Quantum shape-phase transitions in odd-even nuclei are investigated in the framework of the interacting boson-fermion model. Classical and quantum analysis show that the presence of the odd fermion strongly influences the location and nature of the phase transition, especially near the critical point. Experimental evidence for the occurrence of spherical to axially-deformed transitions in odd-proton nuclei Pm, Eu and Tb ($Z=61, 63, 65$) is presented.

Quantum phase transitions (QPTs) are qualitative changes in the ground state properties of a physical system induced by a variation of parameters in the quantum Hamiltonian. These structural modifications have found a variety of applications in diverse areas of physics.¹ One of these applications is to atomic nuclei, where QPTs in even-even nuclei have been extensively investigated (for a review, see²⁻⁴) within the framework of the Interacting Boson Model (IBM),⁵ a model of nuclei in terms of correlated pairs of valence nucleons with $L = 0, 2$ treated as (s, d) bosons.⁵ In the present contribution we extend these studies to odd-even nuclei making use of the Interacting Boson Fermion Model (IBFM),⁶ incorporating an additional unpaired fermion with angular momentum j . The reported results

portray general properties of QPTs in mixed Bose-Fermi systems⁷ and are illustrated for $j = 11/2$.

We consider the Hamiltonian of a system of N monopole (s^\dagger) and quadrupole (d_μ^\dagger) bosons and a single- j fermion ($a_{j,m}^\dagger$)

$$\hat{H} = \hat{H}_B + \hat{H}_F + \hat{V}_{BF} , \quad (1)$$

with

$$\hat{H}_B = \varepsilon_0 \left[(1 - \xi) \hat{n}_d - \frac{\xi}{4N} \hat{Q}^x \cdot \hat{Q}^x \right] , \quad (2a)$$

$$\hat{H}_F = \varepsilon_j \hat{n}_j , \quad (2b)$$

$$\hat{V}_{BF} = \Gamma \hat{Q}^x \cdot (a_j^\dagger \tilde{a}_j)^{(2)} + \Lambda \sqrt{2j+1} : [(d^\dagger \tilde{a}_j)^{(j)} (\tilde{d} a_j^\dagger)^{(j)}]^{(0)} : . \quad (2c)$$

Here $\hat{n}_d = d^\dagger \cdot \tilde{d}$ and \hat{n}_j are the d -boson and fermion number operators respectively, and $\hat{Q}^x = (d^\dagger s + s^\dagger \tilde{d})^{(2)} + \chi (d^\dagger \tilde{d})^{(2)}$. The parameter ε_0 is the scale of the boson energy, ε_j is the energy of the single fermion, Γ and Λ are, respectively, the strengths of the quadrupole and exchange Bose-Fermi interactions. QPTs of the purely bosonic part of the Hamiltonian \hat{H}_B have been extensively investigated.²⁻⁴ There are two control parameters ξ and χ . For fixed χ , as one varies ξ , $0 \leq \xi \leq 1$, the bosonic system undergoes a QPT. The phase transition is first order for $\chi \neq 0$ and becomes second order at $\chi = 0$. No phase transition occurs as a function of χ . In this contribution, we take $\chi = -\frac{\sqrt{7}}{2}$, in which case the spherical phase has U(5) symmetry ($\xi = 0$) and the axially-deformed phase has SU(3) symmetry ($\xi = 1$).⁵ The critical point, separating the two phases occurs at $\xi_c \cong 1/2$.

A complete study of the properties of quantum phase transitions necessitates both a classical and a quantal analysis. A classical analysis amounts to constructing the combined Bose-Fermi potential energy surface (Landau potential) and minimizing it with respect to the classical variables. To this end, we introduce a boson condensate⁵

$$|N; \beta, \gamma\rangle = (N!)^{-1/2} [b_c^\dagger(\beta, \gamma)]^N |0\rangle , \quad (3)$$

$b_c^\dagger = (1 + \beta^2)^{-1/2} [\beta \cos \gamma d_0^\dagger + \beta \sin \gamma (d_2^\dagger + d_{-2}^\dagger) / \sqrt{2} + s^\dagger]$, in terms of the classical variables β, γ . By integrating out the boson degrees of freedom, i.e., by taking the expectation value of \hat{H} (1) in the boson condensate, $\mathcal{H}(N; \beta, \gamma) = \langle N; \beta, \gamma | \hat{H} | N; \beta, \gamma \rangle$, one obtains the fermion Hamiltonian

$$\mathcal{H}(N; \beta, \gamma) = E_B(N; \beta, \gamma) + \varepsilon_j \hat{n}_j + \sum_{m_1, m_2} g_{m_1, m_2}(N; \beta, \gamma) a_{j, m_1}^\dagger a_{j, m_2} , \quad (4)$$

where $E_B = \langle N; \beta, \gamma | \hat{H}_B | N; \beta, \gamma \rangle$. The matrix $g_{m_1, m_2}(N; \beta, \gamma)$ is a real, symmetric matrix, which depends on the Bose-Fermi couplings, Γ and Λ .

Its numerical diagonalization yields the single particle eigenvalues $e_i(\beta, \gamma)$ and eigenfunctions $\psi_i(\beta, \gamma)$, $i = 1, 2, \dots, j + \frac{1}{2}$. These are the single-particle levels in the deformed (β, γ) field generated by the bosons. For $\gamma = 0^\circ$ the eigenvalues are given in explicit analytic form⁸

$$\lambda_K(\beta) = -N\Gamma \left\{ \left(\frac{\beta}{1+\beta^2} \right) \sqrt{5} \left(2 - \beta\chi\sqrt{\frac{2}{7}} \right) P_j[3K^2 - j(j+1)] \right\} \\ - N\Lambda \left\{ \left(\frac{\beta^2}{1+\beta^2} \right) (2j+1)P_j^2[3K^2 - j(j+1)]^2 \right\}, \quad (5)$$

where $P_j = [(2j-1)j(2j+1)(j+1)(2j+3)]^{-1/2}$. The eigenvalues can be labelled by the angular momentum projection on the intrinsic axis $\hat{3}$, $K_3 \equiv K = \frac{1}{2}, \frac{3}{2}, \dots, j$ and they are doubly degenerate. Similarly, the eigenvalues for $\gamma = 60^\circ$ (oblate axial symmetry), are given by $\omega_{K_2}(\beta) = \lambda_{K_3 \rightarrow K_2}(-\beta)$, where K_2 is the corresponding projection on the axis $\hat{2}$. Once the eigenvalues have been obtained, one can calculate the total energy functional (Landau potential for the combined Bose-Fermi system)

$$E_i(N; \beta, \gamma; \xi, \chi; \Gamma, \Lambda) = E_B(N; \beta, \gamma; \xi, \chi) + \varepsilon_j + e_i(N; \beta, \gamma; \chi; \Gamma, \Lambda). \quad (6)$$

Minimization of E_i with respect to β and γ gives the equilibrium values β_e, γ_e (the classical order parameters) for each state. In general, $E_B \propto N^2$ and $e_i \propto N$, however, as shown below, contrary to naive expectations, the odd fermion greatly influences the phase transition.

To facilitate the study of QPTs in the IBFM we set⁹ $\Gamma = -2\varepsilon_0 \frac{\xi}{4N} Q_{jj}$ with $Q_{jj} = \langle j || Y^{(2)} || j \rangle$ and examine the change in (β_e, γ_e) upon variation of the control parameter ξ . For pure quadrupole coupling ($\Lambda = 0$), one can see from the left panel of Fig. 1 that the phase transition is washed out for states 1,2,3 and enhanced for states 4,5,6. The critical point is approximately at the same location as for the purely bosonic case ($\xi_B^c \sim 0.51$) for state 4 ($\xi_4^c \sim 0.50$), but it is moved to larger values for state 5 ($\xi_5^c \sim 0.53$) and state 6 ($\xi_6^c \sim 0.58$). The values of γ_e below and around the critical point are no longer zero. After the critical point, all states become those of a single particle in an axially deformed field ($\gamma_e = 0^\circ$) with equal deformation $\beta_{e,i} = \beta_{e,B}$ ($\beta_{e,B}$ being the equilibrium deformation of E_B). States in this region can be labelled by $K = \frac{1}{2}, \frac{3}{2}, \dots, \frac{11}{2}$, corresponding to states $i = 1, \dots, 6$. The equilibrium values when $\Lambda = -0.287$ are shown in the right panel of Fig. 1. We see that the modifications induced by the presence of a fermion to the phase transition are more dramatic when the exchange interaction is added, especially in the location of the critical point ξ_i^c . The state 6 moves considerably to the right of ξ_B^c . In summary, QPTs in the presence of an

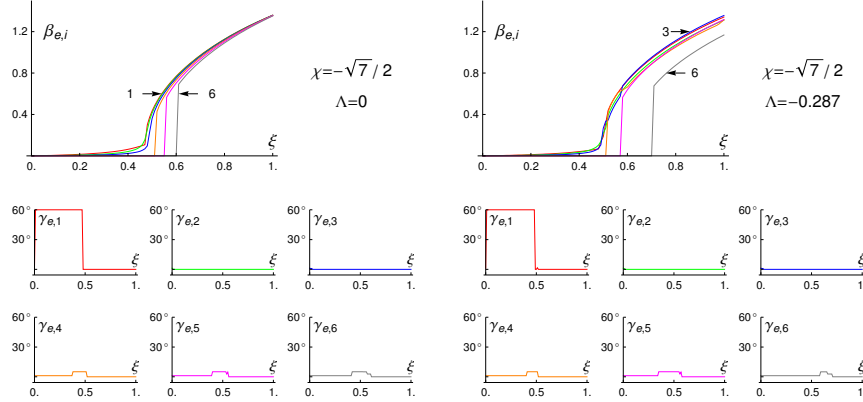


Fig. 1. Equilibrium values, $\beta_{e,i}$ (top part) and $\gamma_{e,i}$ (bottom part) as a function of the control parameter ξ in the U(5)-SU(3) transition ($\chi = -\frac{\sqrt{7}}{2}$), and $N = 10$. Left: $\Lambda = 0$. Right: $\Lambda = -0.287$. States are labelled by the index $i = 1, \dots, 6$.

odd fermion have a different behavior as a function of the control parameter ξ than in the purely bosonic system. The odd fermion acts as a catalyst for some states and as a retardative for others.

The quantal analysis of QPTs is done by diagonalizing numerically the Hamiltonian (1) for finite N . In the semi-microscopic version of the IBFM, the Bose-Fermi interactions are given in terms of the BCS occupation probabilities, u_j and v_j , with $u_j^2 + v_j^2 = 1$. Specifically, $\Gamma = \Gamma_s 2(u_j^2 - v_j^2) Q_{jj}$, $\Lambda = -\Lambda_s 8\sqrt{5}u_j^2v_j^2Q_{jj}^2/(2j+1)$ and we set $\Gamma_s = \frac{\xi}{4N}\epsilon_0$. The correlation diagrams for pure quadrupole coupling ($\Lambda = 0$) are presented in Fig. 2. They describe how the energy levels evolve from the U(5) phase to the SU(3) phase. They also display particle-hole conjugation, that is the transformation ($u \leftrightarrow v$). As quantal order parameters we consider here the expectation value of \hat{n}_d in the states $i = 1, \dots, 6$,

$$\nu_i^{(1)} = \frac{\langle \Psi_i | \hat{n}_d | \Psi_i \rangle}{N}. \quad (7)$$

This is shown in Fig. 3 top part. Since the order parameters $\nu_i^{(1)}$ are related to the square of the classical order parameters $\beta_{e,i}$, this figure is related to Fig. 1 to which it corresponds in the limit $N \rightarrow \infty$. The derivative of $\nu_1^{(1)}$ in the ground state, $\frac{\partial \nu_1^{(1)}}{\partial \xi}$ is also shown in Fig. 3 bottom part. (This quantity diverges when $N \rightarrow \infty$). From this figure one sees clearly that the transition is made sharper by the presence of the fermion for some states,

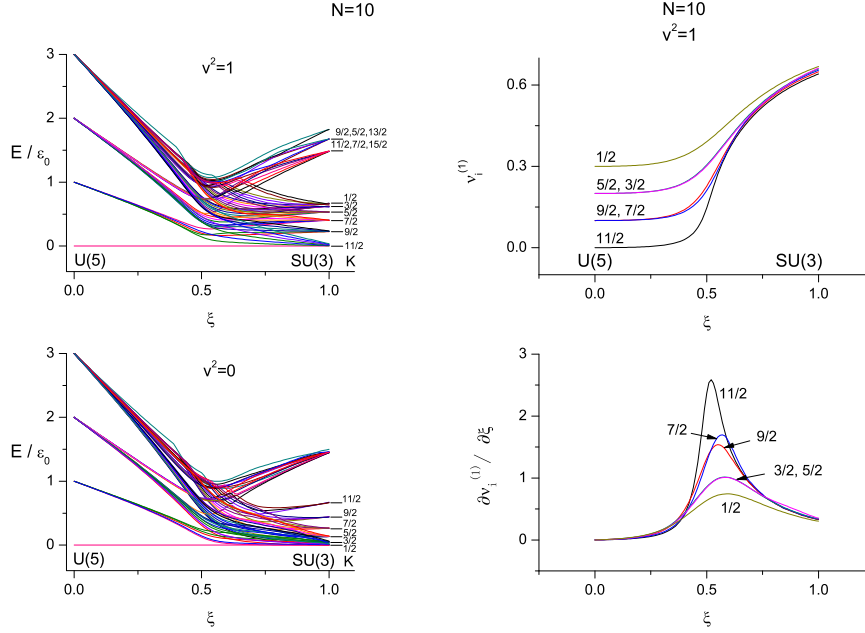


Fig. 2. Correlation diagram for a $j = 11/2$ particle coupled to a system of (s, d) bosons undergoing a U(5)-SU(3) phase transition. Top part $v^2 = 1$, bottom part $v^2 = 0$. The interaction is purely quadrupole.

Fig. 3. The quantal order parameters, $\nu_i^{(1)}$, Eq. (7) (top part), and its derivative, (bottom part), for yrast states with $J = \frac{11}{2}, \dots, \frac{1}{2}$, as a function of the control parameter, ξ . Here $N = 10$ and $v^2 = 1$.

$11/2, 9/2, 7/2$, while is made smoother for others, $5/2, 3/2, 1/2$, a result already seen in the classical analysis.

One of the experimental signatures of QPT in nuclei is the two-neutron separation energies, $S_{2n} = -[E_0(N+1) - E_0(N)]$, which can be related to the derivative of the ground state energy, E_0 , with respect to the control parameter, $\frac{\partial E_0}{\partial \xi}$. S_{2n} can be written as a smooth contribution linear in the boson number N , plus the contribution of the deformation⁵

$$S_{2n} = -A_{2n} - B_{2n}N + S(2n)_{\text{def}}. \quad (8)$$

In order to emphasize the occurrence of the phase transition it is convenient to plot the deformation contribution only, obtained from the data by subtracting the linear dependence, as a function of N . In previous studies of the purely bosonic part it has been shown that N is approximately proportional to the control parameter ξ .² The experimental values of $S(2n)_{\text{def}}$ are

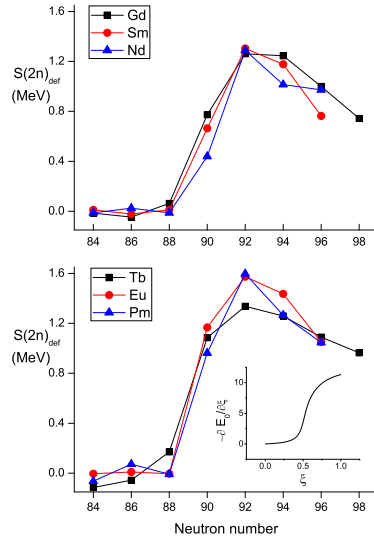


Fig. 4. The contribution of deformation to the two-neutron separation energies, $S(2n)_{\text{def}}$ for even-even ${}_{60}\text{Nd}$ - ${}_{62}\text{Sm}$ - ${}_{64}\text{Gd}$ nuclei (top) and odd-even ${}_{61}\text{Pm}$ - ${}_{63}\text{Eu}$ - ${}_{65}\text{Tb}$ nuclei (bottom), plotted as a function of neutron number. The contribution is enhanced in odd-even nuclei by approximately 300 keV (at neutron number 92). Also the rise between neutron numbers 88 and 90 is sharper in odd-even nuclei than in even-even nuclei. In the limit $N \rightarrow \infty$ (no finite size scaling) the quantity $S(2n)_{\text{def}}$ should be zero before the critical value and finite and large after that. The expected behaviour of $-\frac{\partial E_0}{\partial \xi}$ for the U(5)-SU(3) transition and $N = 10$ is shown in the inset.

shown in the top part of Fig. 4 for even-even nuclei (purely bosonic) and in the bottom part for odd-even nuclei (bosonic plus one fermion). They are obtained from the empirical data with $A_{2n} = -14.61, -15.82, -16.997$ MeV for Nd-Sm-Gd, respectively, and $B_{2n} = 0.657$ MeV, and with $A_{2n} = -15.185, -16.37, -17.672$ MeV for Pm-Eu-Tb, and $B_{2n} = 0.670$ MeV. Precursors of the phase transition are visible in all six nuclei between neutron numbers 88 and 90 in both, and, most importantly, appears to be enhanced in odd-even nuclei relative to the even-even case.

This work was supported in part by the U.S.-Israel Binational Science Foundation and in part by DOE Grant No. DE-FG-02-91ER40608.

References

1. *Understanding Quantum Phase Transitions*, L. Carr, ed., CRC press (2010).
2. F. Iachello, *Rivista Nuovo Cimento* **34**, 617 (2011).
3. P. Cejnar, J. Jolie and R.F. Casten, *Rev. Mod. Phys.* **82**, 2155 (2010).
4. F. Iachello and M.A. Caprio, in Ref. 1, p. 673.
5. F. Iachello and A. Arima, *The Interacting Boson Model* (Cambridge University Press, Cambridge, 1987).
6. F. Iachello and P. Van Isacker, *The Interacting Boson-Fermion Model* (Cambridge University Press, Cambridge, 1991).
7. D. Petrellis, A. Leviatan and F. Iachello, *Ann. Phys. (NY)* **326**, 926 (2011).
8. A. Leviatan, *Phys. Lett. B* **209**, 415 (1988).
9. C.E. Alonso, J.M. Arias, L. Fortunato and A. Vitturi, *Phys. Rev. C* **72**, 061302(R) (2005).